Carcinogenesis vol.34 no.9 pp.2156–2169, 2013
doi:10.1093/carcin/bgt159
Advance Access publication May 13, 2013

SB365, *Pulsatilla* saponin D, targets c-Met and exerts antiangiogenic and antitumor activities

Sang-Won Hong[†], Kyung Hee Jung[†], Hee-Seung Lee, Mi Kwon Son, Hong Hua Yan, Nam Sook Kang[1], Jongkook Lee[2] and Soon-Sun Hong*

Department of Biomedical Sciences, College of Medicine, Inha University, 3-ga, Sinheung-dong, Jung-gu, Incheon 400-712, Republic of Korea, [1]Graduate School of New 1Drug Discovery & Development, Chungnam National University, Daejeon 305-764, Republic of Korea and [2]College of Pharmacy, Kangwon National University, Chuncheon, Gangwon-do 200-701, Republic of Korea

*To whom correspondence should be addressed. Tel: +82 32 890 3683; Fax: +82 32 890 2462;
Email: hongs@inha.ac.kr

SB365, *Pulsatilla* saponin D isolated from the root of *Pulsatilla koreana*, has exhibited potential beneficial effects as a chemopreventive agent for critical health conditions including cancer. However, the molecular mechanisms underlying the activity of SB365 remain unknown. Here, we examined anticancer efficacy of SB365 against gastric cancer and its mechanism of action. SB365 effectively inhibited the growth of gastric cancer cells. Its apoptotic effect was accompanied by increased evidence of cleaved caspase-3 and poly(ADP ribose) polymerase. To elucidate the anticancer mechanism of SB365, we used an array of 42 different receptor tyrosine kinases (RTKs). Of the 42 different phospho-RTKs, SB365 strongly inhibited expression of activated c-mesenchymal–epithelial transition factor (c-Met) in gastric cancer cells. Also, the activation of the c-Met signal cascade components, including Akt and mammalian target of rapamycin, was inhibited by SB365 in a dose-dependent manner. In angiogenesis studies, SB365 inhibited tube formation in hepatocyte growth factor (HGF)-induced human umbilical vein endothelial cells and suppressed microvessel sprouting from the rat aortic ring, *ex vivo*, and blood vessel formation in the Matrigel plug assay in mice. In xenograft animal models, SB365 significantly delayed tumor growth in a dose-dependent manner. In tumor tissue, SB365 suppressed c-Met signaling, proliferation and angiogenesis and induced apoptosis. These findings suggest that SB365 docks at an allosteric site on c-Met and thereby targets c-Met signaling pathway, cell growth/angiogenesis inhibition and apoptosis induction. Therefore, SB365 may be a novel drug candidate for the treatment of gastric cancer.

Introduction

Gastric cancer is one of the most common malignancies and remains the second leading cause of cancer-related mortality worldwide (1). Despite radical surgery, major obstacles such as local invasion and metastasis result in a very low cure rate. Indeed, over 20% of gastric cancer patient show peritoneal and liver metastasis at surgery, and 30% of those who die from gastric cancer have peritoneal dissemination (2,3). Nevertheless, standard therapy for gastric cancer has not yet been established. Safer and more effective therapeutic strategies and the identification of new molecular targets for gastric cancer treatment, based on understanding the underlying mechanism, are urgently needed.

The c-mesenchymal–epithelial transition factor (c-Met) is the prototypical member of a subfamily of receptor tyrosine kinases (RTKs). In physiological conditions, c-Met is mainly activated by its only known high-affinity ligand, hepatocyte growth factor (HGF), also known as scatter factor (4). The c-Met pathway is one of the most frequently deregulated pathways in human cancer, and aberrant c-Met signaling has been documented in many solid tumors (5). Activation of c-Met regulates many functional responses, including cell proliferation, survival, motility and invasion through the modulation of signaling pathways such as phosphoinositide-3 kinase (PI3K)/Akt, signal transducer and activator of transcription 3 (STAT3) and Ras/Mek (6,7). c-Met mutations have been reported in many cancers, including gastric, head and neck, liver and ovarian cancers, as well as in metastases of some of those cancers (8,9). In addition, c-Met has also been reported to be frequently overexpressed or amplified in many cancers (10–12). In gastric cancer, a common cause for the activation of the c-Met pathway is the amplification of the Met gene, with subsequent proteins overexpression and kinase activation (13). Overexpression of c-Met has been reported in 58.8% of gastric cancer tissue, and c-Met alteration was shown to be related to tumor size and tumor invasion (14). For this reason, c-Met has emerged as an attractive target for therapeutic medication in gastric cancer.

Traditional medicines provide highly fertile ground for modern drug development; however a pathway of discovery, isolation, and mechanism studies must be followed before their development and use in clinical settings (15). *Pulsatilla koreana* belongs to the family Ranunculaceae and its roots have been widely used in treatment of several diseases in Korea (16). In this study, we first isolated various saponins from *P.koreana* to identify a saponin with high efficacy, *Pulsatilla* saponin D (hereafter designated SB365). Saponins have been known to provide a wide range of health benefits and are used as precursors of drugs in the pharmaceutical industry (17,18). In particular, several saponins have been reported to exert anticancer effects, inhibiting cell growth via cell cycle arrest and apoptosis in various cancer cell types (19–21).

Although the physiological and anticancer effects of saponins have previously been documented, the exact signaling mechanism that mediates these effects has not been fully evaluated. In this study, we investigated the anticancer activity of SB365 and mechanism of action of SB365, a potent saponin D. Especially, we have studied the signaling mechanisms that have been attributed to the effects of SB365 in HGF/c-Met pathways involved in gastric cancer. Here, our present study reveals that SB365 induces apoptosis and inhibits proliferation and angiogenesis by inhibiting the HGF/c-Met pathway in gastric cancer.

Materials and methods

Cells and materials

The human gastric cancer cell lines MKN-45, MKN-28 and AGS along with normal human gastric Hs677 cells were purchased from the Korean Cell Line Bank (KCLB, Seoul, Korea). These cells were cultured in RPMI-1640 medium, supplemented with 10% fetal bovine serum (FBS) and 1% penicillin/streptomycin. FBS and all other agents used in cell culture studies were purchased from Invitrogen (Carlsbad, CA). Cultures were maintained at 37°C in a CO_2 incubator in a controlled humidified atmosphere composed of 95% air and 5% CO_2. Human umbilical vein endothelial cells (HUVECs)

Abbreviations: ATP, adenosine triphosphate; BrdU, 5′-bromo-2′-deoxyuridine; c-Met, c-mesenchymal–epithelial transition factor; DAPI, 4′,6-diamidino-2-phenylindole; FBS, fetal bovine serum; 5-FU, 5-fluorourcil; HGF, hepatocyte growth factor; HUVEC, human umbilical vein endothelial cell; mTOR, mammalian target of rapamycin; PBS, phosphate buffered saline; PI3K, phosphoinositide-3 kinase; RTK, receptor tyrosine kinase; STAT3, signal transducer and activator of transcription 3; TUNEL, terminal deoxynucleotidyl transferase-mediated dUTP nick end labeling; VEGF, vascular endothelial growth factor.

[†]These authors contributed equally to this work.

were grown in a gelatin-coated 75 cm^2 flask in M199 medium containing 20 ng/ml basic fibroblast growth factor, 100 U/ml heparin and 20% FBS at 37°C in a humidified atmosphere of 5% CO_2/95% air. The cells used in this study were from passages 5–6. SB365 was isolated from *P.koreana* (Supplementary Materials and methods, available at *Carcinogenesis* Online).

Immunodetection of incorporation of 5′-bromo-2′-deoxyuridine

MKN-45 gastric cancer cells were plated onto 18 mm cover glass in RPMI-1640 medium at ~70% confluence for 24 h. The cells were then treated with SB365 at 10 µM for 2 h and were then pulse-labeled (4 h) with 10 µM 5′-bromo-2′-deoxyuridine (BrdU). After labeling, the cells were washed twice

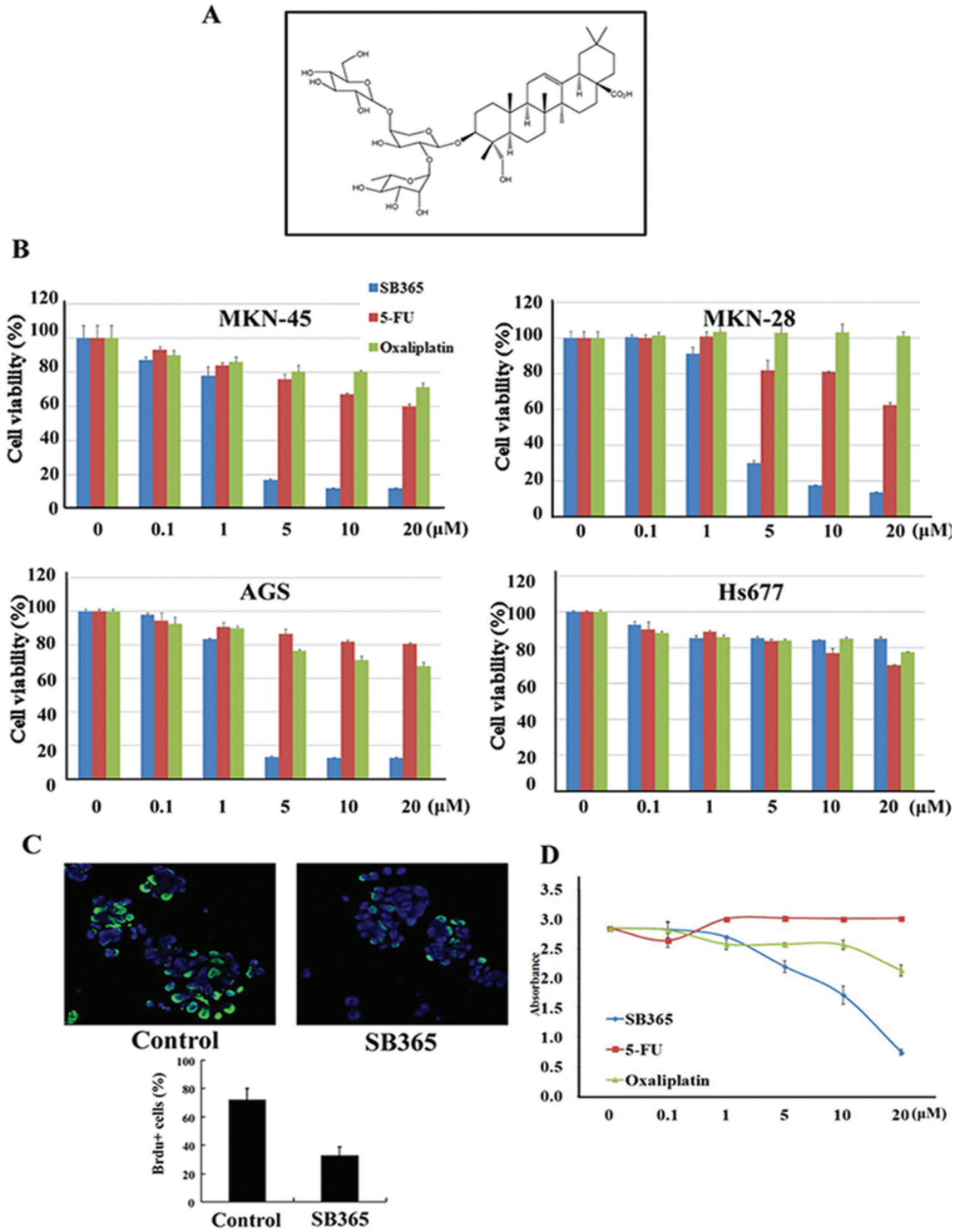

Fig. 1. Chemical structure of SB365 (*Pulsatilla* saponin D) and its effect on the proliferation of human gastric cancer cells. (**A**) Chemical structure of SB365. (**B**) The cytotoxic effects of SB365, 5-FU and oxaliplatin on gastric cancer cells (MKN-45, MKN-28 and AGS) and Hs677 normal gastric cells were measured by the 3-(4,5-dimethylthiazole-2-yl)-2,5-diphenyl tetrazolium bromide assay for 48 and 24 h, respectively. (**C**) BrdU staining along with DAPI counter staining in MKN-45 gastric cancer cells. (**D**) Proliferation of MKN-45 gastric cancer cells assessed by BrdU proliferation enzyme-linked immunosorbent assay. Results are expressed as percent cell proliferation relative to that of control. Data represent mean ± SD from the triplicate wells.

with phosphate buffered saline (PBS) and fixed in ice-cold 1% paraformaldehyde and then washed with PBS to remove organic solvent. Fluorescein isothiocyanate-labeled anti-BrdU antibody, diluted with PBS buffer containing 0.1% Triton X-100, was used to measure BrdU incorporation by fluorescence microscopy.

Flow cytometry analysis

MKN-45 gastric cancer cells were treated with various concentrations of SB365 or 0.1% dimethyl sulfoxide for 48 h. Floating and adherent cells were collected and fixed in cold 70% ethanol at 4°C overnight. After washing with PBS, the cells were stained with propidium iodide and RNase A for 1 h in the dark and subjected to flow cytometric analysis in order to determine the percentage of cells at specific phases of the cell cycle (sub-G_1, G_0/G_1, S and G_2/M). Flow cytometric analysis was performed using a FACSCalibur flow cytometer (Becton Dickinson, San Jose, CA) equipped with a 488 nm argon laser.

Phospho-RTK array analysis

The Human Phospho-RTK Array Kit (R&D Systems, Minneapolis, MN) was used to determine the relative tyrosine phosphorylation of RTKs. The membranes contained spotted antibodies corresponding to 42 distinct RTKs and both positive and negative controls. MKN-45 gastric cancer cells were cultured on a 10 cm dish in RPMI-1640 medium with 10% FBS, changed into the media without FBS for 24 h and lysed in NP-40 lysis buffer. The arrays were blocked in the provided blocking buffer and incubated with 50 µg of cell lysate overnight at 4°C. They were then washed and incubated with a horseradish peroxidase-conjugated detection antibody, treated with enhanced chemiluminescence reagents and exposed to film. The intensity of each spot detected on the phospho-RTK array was measured by Image analyzer, LAS-4000 (Fuji Film, Tokyo, Japan) and intensity of the average signal of the pair of duplicated spots was calculated relative to the negative control spots. Background intensity was also determined and subtracted from each average signal.

Tube formation assay

A 10 mg/ml (200 µl) of Matrigel (BD Biosciences, Franklin Lakes, NJ) was polymerized for 30 min at 37°C. HUVECs were suspended in M199 (2% FBS) medium at a density of 2.5×10^5 cells/ml, and 0.2 ml of cell suspension was added to each well coated with Matrigel, together with or without the indicated concentrations of SB365 and HGF (50 ng/ml) for 14 h. The morphological changes of the cells and tubes formed were observed under a phase-contrast microscope and photographed at ×200 and ×400 magnification.

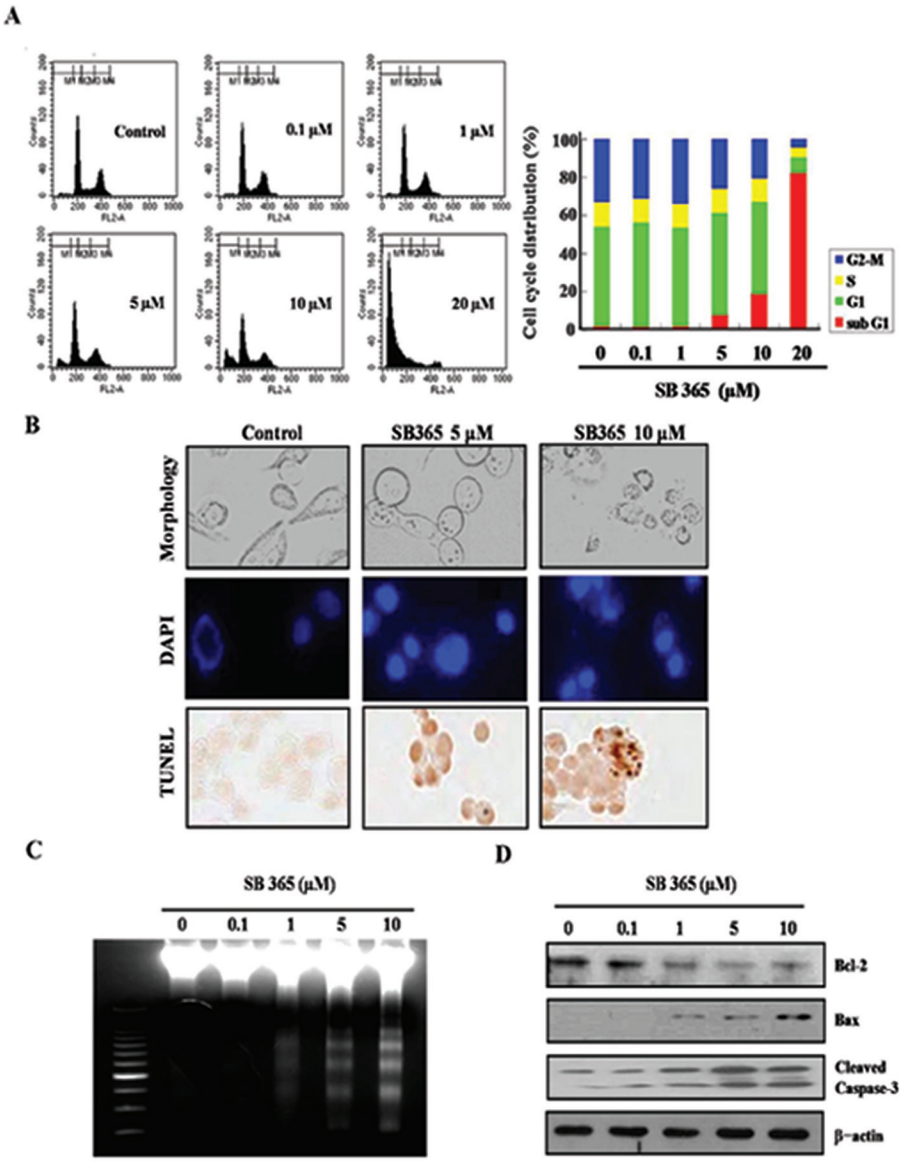

Fig. 2. Effect of SB365 on apoptosis in MKN-45 gastric cancer cells. (**A**) Gastric cancer cells were treated with SB365 (0, 0.1, 1, 5, 10 and 20 µM) for 24 h, stained with propidium iodide and analyzed on a FACSCalibur flow cytometer. (**B**) The induction of apoptosis by SB365 was assessed by DAPI and TUNEL staining, which were photographed at ×400 magnification. (**C**) DNA damage induced by SB365 was detected by a DNA assay. (**D**) The expression of Bcl-2, Bax and cleaved caspase-3 was determined by western blotting in cells treated with SB365 at the indicated doses for 24 h.

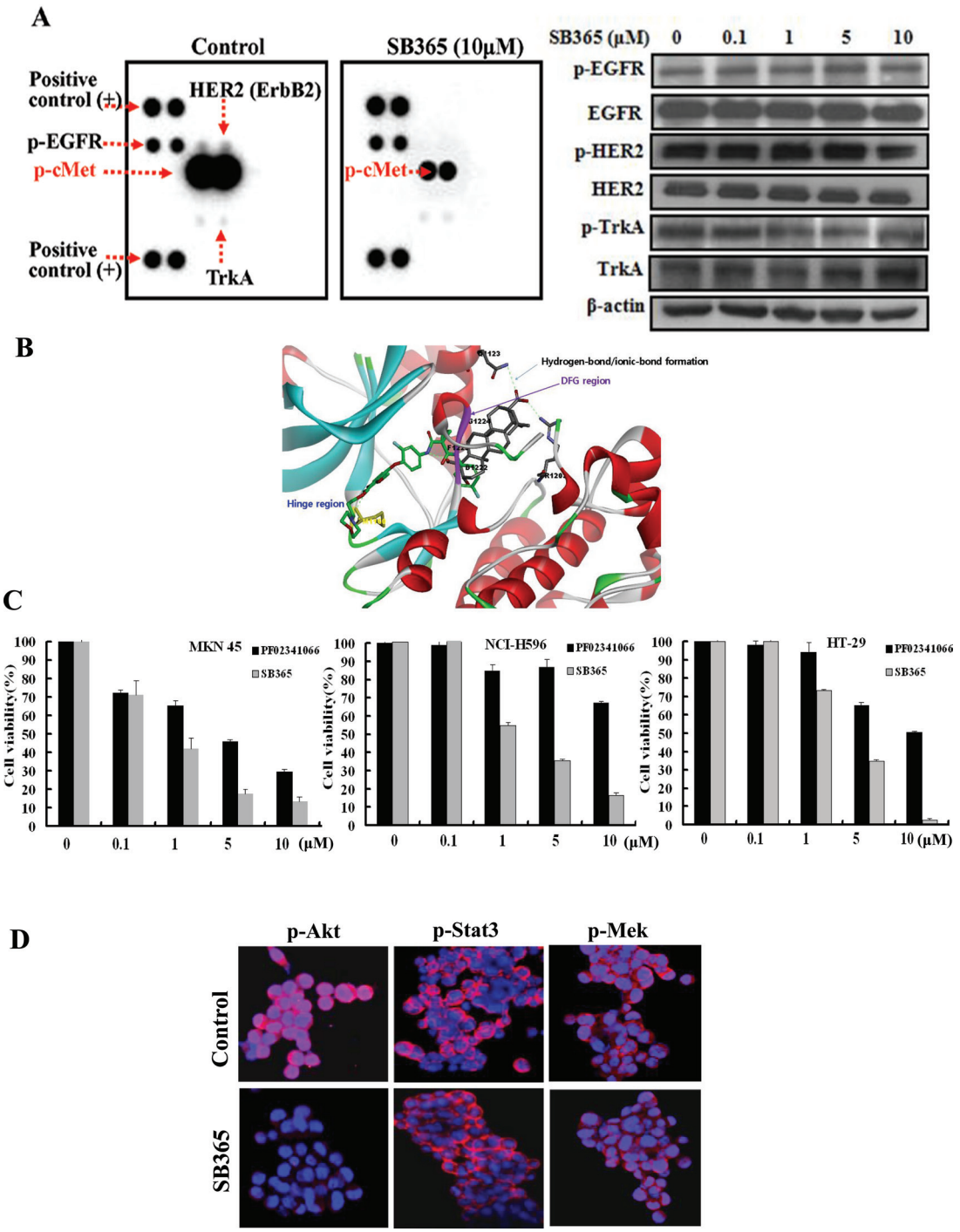

Wounding migration assay

HUVECs plated on 60 mm diameter culture dishes at 90% confluence were wounded with a razor blade score 2 mm in width and marked at the injury line. After wounding, the peeled off cells were removed with a serum-free medium and further incubated in M199 medium with 2% FBS, 1 mM thymidine (Sigma–Aldrich, St Louis, MO), SB365 (0.1–10 μM) and/or HGF (50 ng/ml). HUVECs were allowed to migrate for 24 h and were rinsed with a serum-free medium, followed by fixing with absolute ethanol. Migration was quantitated by counting the number of cells that moved beyond the reference line.

Aortic ring sprouting assay

Aortas were harvested from 6-week-old Sprague Dawley rats. Plates (48-well) were coated with 120 μl of Matrigel; after gelling, the aortic rings were placed in the wells and sealed in place with an overlay of 100 μl of Matrigel. HGF (100 ng/ml) with or without SB365 (1 or 10 μM) was added to the wells in a final volume of 200 μl of human endothelial serum-free medium (Invitrogen). Medium alone was assayed as a control. On day 7, cells were fixed to assess microvessel sprouting and photographed using an Olympus inverted microscope (Olympus, Tokyo, Japan). Six independent experiments were performed. The assay was scored from 0 (least positive) to 5 (most positive) in a double-blinded manner.

Matrigel plug assay

Six-week-old male nude BALB/c mice were obtained from Orient-Bio Laboratory Animal Research Center Co., Ltd (Gyeonggi-do, Kapyung, Korea). The mice were subcutaneously injected with 700 μl of Matrigel containing HGF (300 ng/ml) and either SB365 (10 μM) or PBS (10 μl). After 7 days, the mice were killed and the Matrigel plugs were removed. The resulting functional microvessels with intact red blood cells were quantified using a microscope.

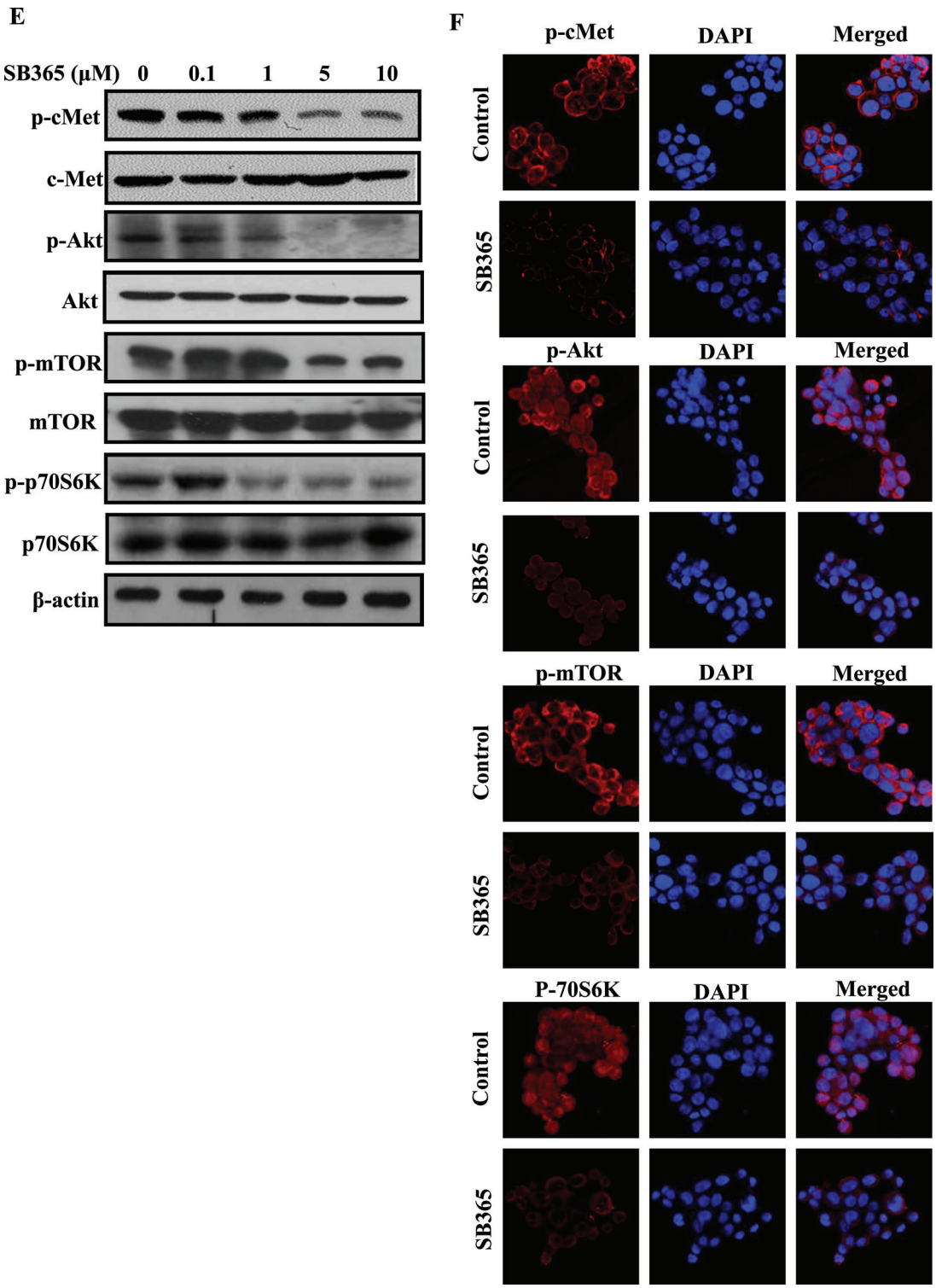

Fig. 3. c-Met inhibition by SB365. (**A**) Phosphorylation of RTKs by SB365 and expression of phospho-human epidermal growth factor receptor 2, phospho-epidermal growth factor receptor and phospho-neurotrophic tyrosine kinase receptor by SB365 in MKN-45 gastric cancer cells. (**B**) Proposed structure for the c-Met complex with the aglycone of SB365 (the original crystal ligand: green; the aglycone of SB365: gray). H-bonding interactions between the aglycone of SB365 and c-Met are shown in green dotted lines. The DFG moiety of c-Met was indicated in a magenta ribbon. (**C**) Effects of SB365 in c-Met alteration cells. The growth of the cells (MKN-45 gastric cancer cells; c-Met amplification cells, NCI-H596 non-small cell lung cancer cells; c-Met splicing mutation cells and HT-29 colon cancer cells; c-Met overexpression cancer cells) were measured by the 3-(4,5-dimethylthiazole-2-yl)-2,5-diphenyl tetrazolium bromide assay. (**D**) Inhibition of p-Akt, p-STAT3 and p-Mek by SB365 in MKN-45 gastric cancer cells. (**E**) Effect of SB36 on the c-Met/AKT/mTOR pathway in MKN-45 gastric cancer cells. The cells were treated with SB365 at various doses (0.1–10 μM). Western blotting experiments for p-Akt, p-mTOR and p-p70S6K were performed with the cell lysates. (**F**) Immunofluorescent imaging at ×400 magnification of c-Met/Akt/mTOR target proteins after treatment with SB365 is shown. Anti-rabbit antibodies against p-Akt, p-mTOR and p-p70S6K were used for labeling. DAPI was used to counter stain the nucleus.

Xenograft mouse model

Animal care and all experimental procedures were conducted in accordance with the approval and guidelines of the Inha Institutional Animal Care and Use Committee (INHA IACUC) at the Medical School of Inha University. The male nude mice (6 weeks old) were randomly divided into three groups (control, 10 mg/kg SB365 and 30 mg/kg SB365). The MKN-45 cells were harvested and mixed with PBS (200 µl/mouse) and then inoculated into a flank of each nude mouse (2×10^6 of MKN-45 cells). When the tumors reached a volume of ~50 mm^3, the mice were given a daily oral dose of SB365 (treated groups) or vehicle only (negative control) for 12 days. The tumor dimensions were measured twice a week using a digital caliper and the tumor volume was calculated using the formula $V = \text{length} \times \text{width}^2 \times 0.5$. A portion of each tumor was fixed in buffered formalin. The remaining tissues were stored at −70°C for future analysis.

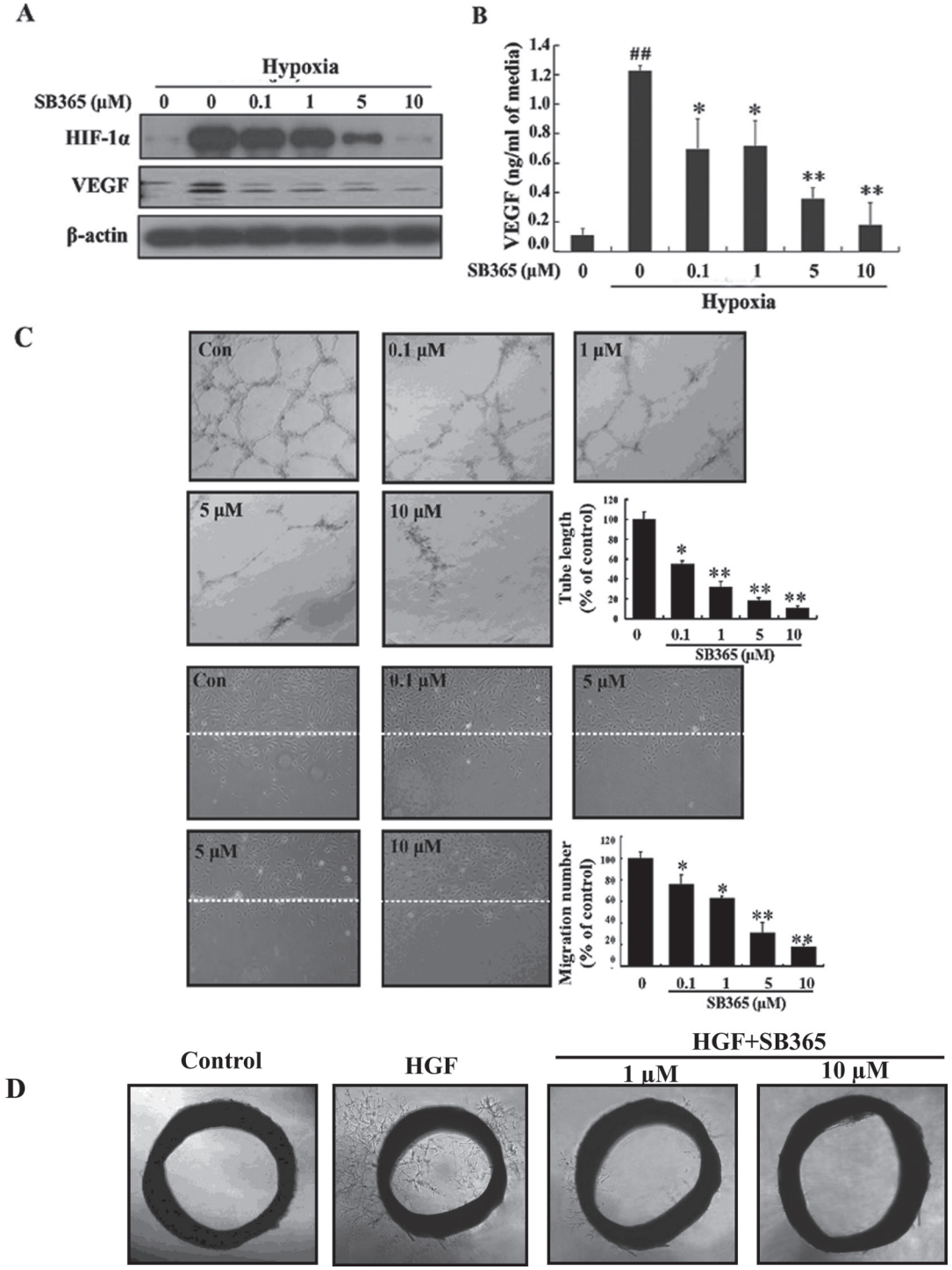

Fig. 4. Effect of SB365 on angiogenesis. (**A**) Inhibition of HIF-1α and VEGF by SB365 in hypoxia-induced MKN-45 gastric cancer cells. (**B**) Production of VEGF by SB365 in MKN-45 gastric cancer cells that were hypoxia-induced for 24 h. Data from the triplicate wells were represented as mean ± SD. $^{\#\#}P < 0.001$, compared with control; $^{*}P < 0.05$ and $^{**}P < 0.01$, compared with hypoxia control. (**C**) Effects of SB365 treatment on HGF-induced tube formation and migration, *in vitro*. Capillary tube formation was assessed after 18 h. The morphological changes in the cells and tube formations were observed under a phase-contrast microscope and photographed at ×200 magnification. For migration, HUVECs were plated at 90% confluence and scratched with a razor blade. $^{*}P < 0.05$ and $^{**}P < 0.01$, compared with control. (**D**) Effects of SB365 on the *ex vivo* HGF-induced microvessel sprouting assay. Representative photographs of sprouts from the margins of aortic rings.

Statistical analysis

Data are expressed as mean ± SD. Statistical analysis was performed using analysis of variance and an unpaired Student′s *t*-test. A *P*-value of 0.05 or less was considered statistically significant. Statistical calculations were performed using SPSS software for Windows operating system (Version 10.0; SPSS, Chicago, IL).

Results

SB365 inhibits the growth and proliferation of gastric cancer cells

To evaluate the inhibitory effect of SB365 on the growth of gastric cancer cells, three cell lines (MKN-45, MKN-28 and AGS) were used. The cells were exposed to various concentrations of SB365, 5-fluorouracil (5-FU) and oxaliplatin (conventional anticancer drugs of gastric cancer) for 48 h. The SB365 treatment reduced the cell viability in all gastric cancer cell lines in a dose-dependent manner (Figure 1B). Further, when we compared the growth of gastric cancer cells after treatment with SB365, 5-FU and oxaliplatin at five concentrations (0.1–20 μM), SB365 treatment caused the greatest reduction in the growth rate of the gastric cancer cells, strongly inhibiting 80–90% of cell growth at dose of 5 μM, indicating that SB365 is more effective than 5-FU and oxaliplatin in gastric cancer cells. More important thing was that SB365 inhibited specifically cell growth of gastric cancer cells without cytotoxicity in Hs677 normal gastric cells. To confirm the effect of SB365 on cell response, the level of incorporation of BrdU was measured using BrdU staining and a cell proliferation assay. As shown in Figure 1C, SB365 strongly inhibited cell proliferation of MKN-45 gastric cancer cells. In addition, the antiproliferative effect of SB365 was more potent than those of 5-FU and oxaliplatin (Figure 1D).

SB365 induces apoptosis in gastric cancer cells

To identify the apoptotic effect of SB365 in MKN-45 gastric cancer cells, we used flow cytomertry, 4′,6-diamidino-2-phenylindole (DAPI) staining, terminal deoxynucleotidyl transferase-mediated dUTP nick end labeling (TUNEL) assay, DNA fragmentation and western blot. As observed by flow cytometry analysis, treatment with SB365 (0.1–20 μM) increased sub-G_1 phase by 80% (Figure 2A).

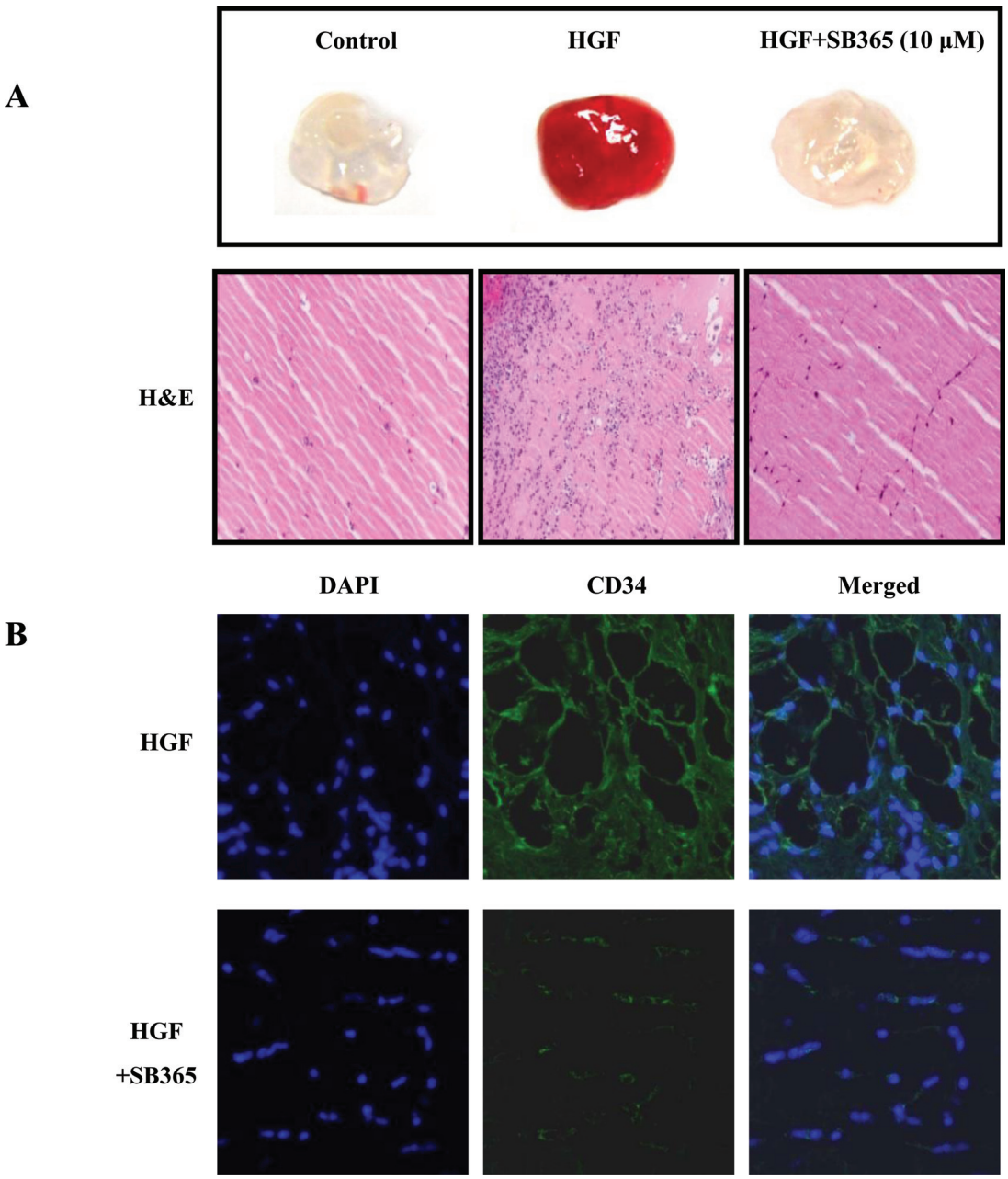

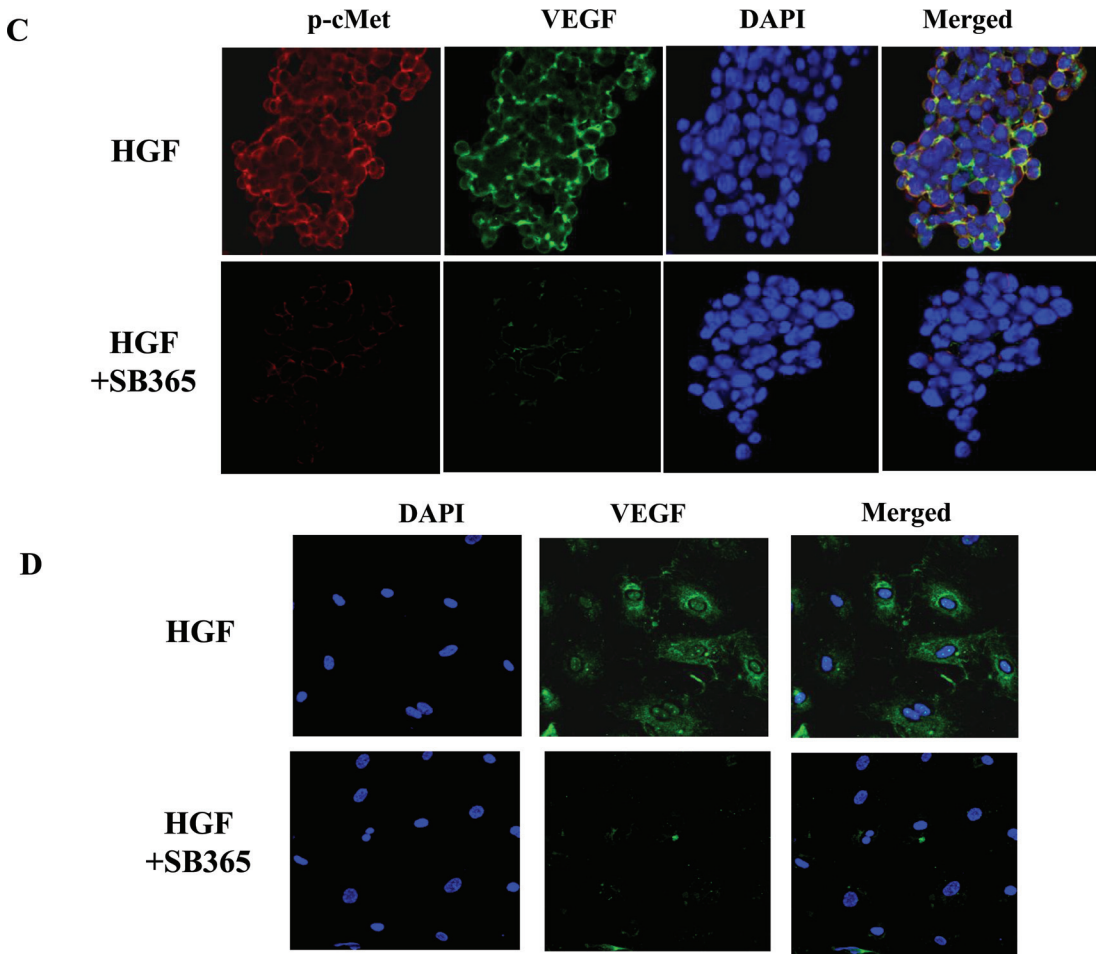

Fig. 5. Antiangiogenic effect of SB365 in the Matrigel plug assay *in vivo* and HGF-induced gastric cancer cells and HUVECs. (**A**) Matrigel plugs with HGF (300 ng/ml) and/or SB365 (10 μM) were implanted into mice and photographed after 7 days to show the extent of vascularization. The plugs were sectioned and stained with hematoxylin and eosin. The infiltrating microvessels with intact red blood cell were quantified. (**B**) Endothelial cells in the plug were immunostained with the CD34. A stained plug was observed by microscopy at ×400 magnification. (**C**) Expression of c-Met and VEGF by SB365 in HGF-induced MKN-45 gastric cancer cells. (**D**) Expression of VEGF by SB365 in HGF-induced HUVECs.

DAPI staining showed that nuclear condensation and perinuclear apoptotic bodies were produced after treatment with SB365 (5 and 10 μM). Apoptosis due to SB365 treatment was confirmed by the detection of DNA fragmentation using TUNEL staining and the DNA fragmentation assay (Figure 2B and C). Further, SB365 treatment in MKN-45 gastric cancer cells increased their expression of cleaved caspase-3 and Bax and decreased that of Bcl-2 (Figure 2D). These results show that SB365 induces cell apoptosis in a dose-dependent manner.

c-Met is highly phosphorylated in MKN-45 gastric cancer cells and suppressed by SB365

To better understand the anticancer effect of SB365, we carried out a human phospho-RTK array containing 42 RTKs to investigate the relative levels of phosphorylation of different RTKs. As seen in Figure 3A, we detected that not only c-Met but also human epidermal growth factor receptor 2 (or ErbB2), epidermal growth factor receptor and neurotrophic tyrosine kinase receptor were activated in MKN-45 gastric cancer cells. In particular, c-Met was highly phosphorylated in MKN-45 gastric cancer cells; however, SB365 strongly inhibited the phosphorylation of c-Met. This was confirmed by the result that SB365 did not affect inhibition of human epidermal growth factor receptor 2, epidermal growth factor receptor and neurotrophic tyrosine kinase receptor phosphorylation in a dose–response by western blotting. This indicates that SB365 may be a possible inhibitor of c-Met in gastric cancer cells.

Structure of SB365 in complex with Met and effect of SB365 on cells with c-Met alteration

To further dissect the interaction of SB365 with c-Met, we established the binding mode for the c-Met–SB365 complex using molecular modeling techniques (Figure 3B). Modeling experiments suggested that the aglycone of SB365 (gray compound) would dock into an allosteric site in c-Met, which is created by an inactive 'DFG-out' conformation. This analysis utilized a crystal structure of c-Met that was obtained from the Protein Data Bank (pdb entry: 3LQ8) (22). Calculations for this docking analysis were carried out using LibDock (23) interfaced with Discovery Studio 3.0 (Accelrys, San Diego, CA). The crystal structure of 3LQ8 was regenerated very well with a root mean square displacement of 0.7 Å. For self-docking of the original crystal ligand (XL-880: green) onto 3LQ8, we obtained a well-superimposed conformation from the original crystal structure (Dock_Score value, 170.0 kcal/mol). Based on the self-docking model, the aglycon of SB365 (gray) is bound in an allosteric site in c-Met (Dock_Score value, 110.0 kcal/mol). The carboxylic group of SB365 interacts through ionic interaction with $–NH_2$ in Q1123 and $–NH_3^+$ in R1203. Hydrophobic interactions of SB365 with c-Met around the Asp-Phe-Gly (DFG) moiety may also contribute to the c-Met affinity of SB365. It is likely that the low dock score compared with that of the original ligand arises from the absence of hinge-binding interactions between c-Met and the aglycone of SB365. To further confirm the c-Met inhibition of SB365, we compared cell growth with SB365 and a well-known c-Met inhibitor PF-02341066 in various

c-Met alteration cells including MKN-45 (c-Met amplification), NCI-H596 (c-Met splicing mutation) and HT-29 (c-Met overexpression) cells. Interestingly, SB365 equally inhibited the growth of all three cell types, whereas PF-02341066 only inhibited cell growth in the c-Met amplified MKN-45 cells in a dose-dependent manner (Figure 3C).

SB365 inhibits the c-Met/Akt/mTOR signaling pathway in MKN-45 gastric cancer cells

The c-Met has been reported to control a range of diverse cellular processes such as cell proliferation, differentiation, transformation and apoptosis through the modulation of the PI3K/Akt/mammalian target of rapamycin (mTOR), STAT3 and Ras/Mek signaling pathways (24–26). Therefore, to elucidate the mechanism responsible for c-Met inhibition by SB365, we tested whether SB365 inhibited the expression of p-Akt, p-STAT3 and p-Mek, which are representative downstream molecules of the PI3K/Akt/mTOR, STAT3 and Ras/Mek signaling pathways, respectively (Figure 3D). Interestingly, SB365 inhibited the expression of p-Akt in MKN-45 gastric cancer cells, suggesting that c-Met inhibition of SB365 may be through the PI3K/Akt/mTOR signaling pathway. To further identify the effect of SB365 on c-Met/Akt/mTOR pathway in MKN-45 gastric cancer cells, we investigated the expression of c-Met, Akt, mTOR and p70S6K. When gastric cancer cells were treated with various concentrations of SB365 for 24 h, the phosphorylation levels of Akt and its downstream factor mTOR were effectively suppressed (Figure 3D and E). mTOR activation results in the phosphorylation of effectors such as p70S6K, leading to mTOR-dependent gene transcription, which in turn regulates cell proliferation and protein synthesis (27). To further confirm these results, we conducted confocal fluorescent microscopy analysis. In agreement with the western blotting results, SB365 obviously reduced the expression of p-cMet, p-Akt, p-mTOR and p-p70S6K in MKN-45 gastric cancer cells (Figure 3F).

SB365 inhibits the expression of HIF-1α and vascular endothelial growth factor in MKN-45 gastric cancer cells

As HIF-1α is stabilized in hypoxic conditions and increases angiogenic signals such as vascular endothelial growth factor (VEGF) (28), we examined HIF-1α and VEGF expression in MKN-45 gastric cancer cells treated with various concentrations of SB365 under hypoxia-mimicking conditions, induced by treatment with 100 μM $CoCl_2$ for 6 h. As shown in Figure 4A, the HIF-1α expression increased in the hypoxic conditions. However, SB365 inhibited the hypoxia-induced HIF-1α expression, starting at a concentration of 0.1 μM. To further examine the effect of SB365 on hypoxia-induced VEGF, an immediate downstream target gene of HIF-1α, VEGF protein levels were evaluated by western blotting and enzyme-linked immunosorbent assay in MKN-45 gastric cancer cells. An increase in VEGF expression was observed under hypoxic conditions, and the SB365 treatment was found to suppress VEGF expression and production in a dose-dependent manner ($P < 0.05$, Figure 4A and B).

SB365 suppressed HGF-induced tubular structure formation and migration in HUVECs

In order to assess the antiangiogenic property of SB365, we carried out a capillary tube formation and migration assay using HUVECs, a well-known *in vitro* angiogenesis model. HUVECs were activated by HGF treatment and then treated with various concentrations (0.1–10 μM) of SB365 for 18 h. Tube formation was visualized under a microscope and photographed. When the HUVECs were seeded on Matrigel, robust tubular-like structures formed in the presence of HGF. However, treatment with 0.1–10 μM of SB365 significantly suppressed or terminated the HGF-induced formation of vessel-like structures as observed by the elongation and alignment of the cells at the indicated concentrations (Figure 4C). Cell migration is critical for endothelial cells to form blood vessels in angiogenesis and is necessary for tumor growth and metastasis. Thus, we conducted a wound migration assay to identify the effect of SB365 on cell migration. When the endothelial cells were wounded and incubated in a medium with HGF in the presence of SB365 for 24 h, SB365 inhibited remarkably HGF-induced cell migration (Figure 4C). Considering that endothelial migration and tube formation are highly relevant properties in the process of angiogenesis, our results show that SB365 has the ability to block HGF-induced angiogenesis *in vitro*.

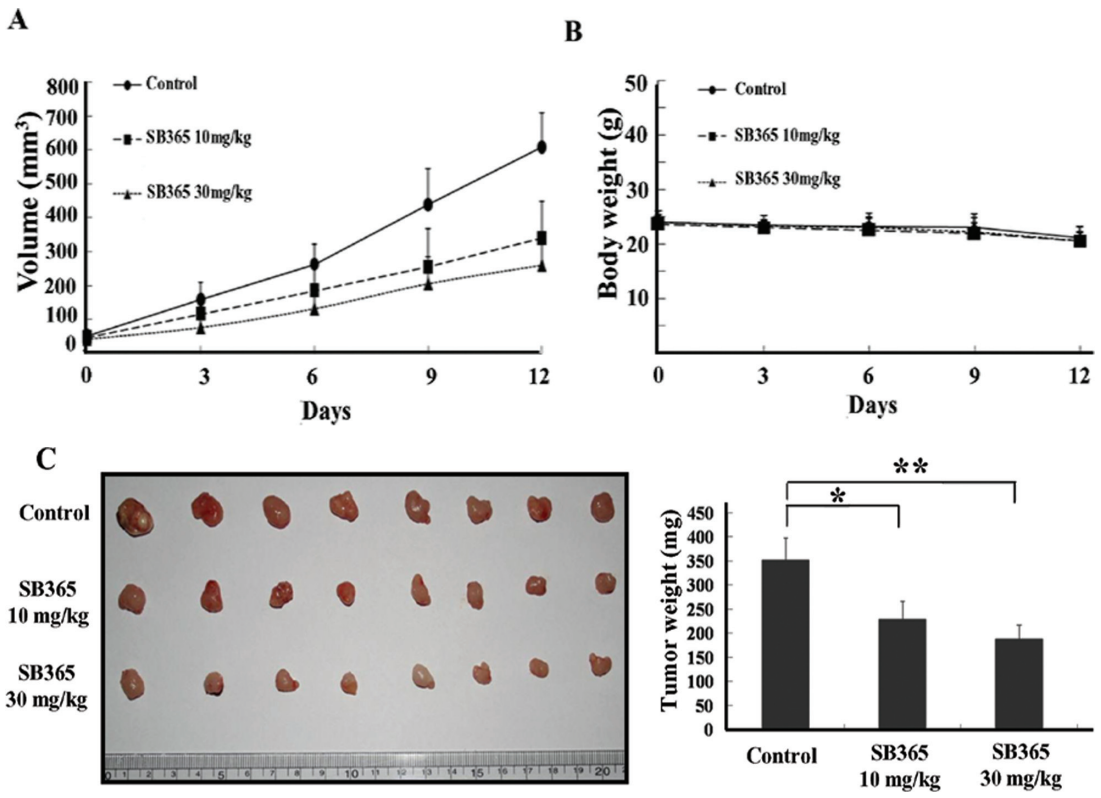

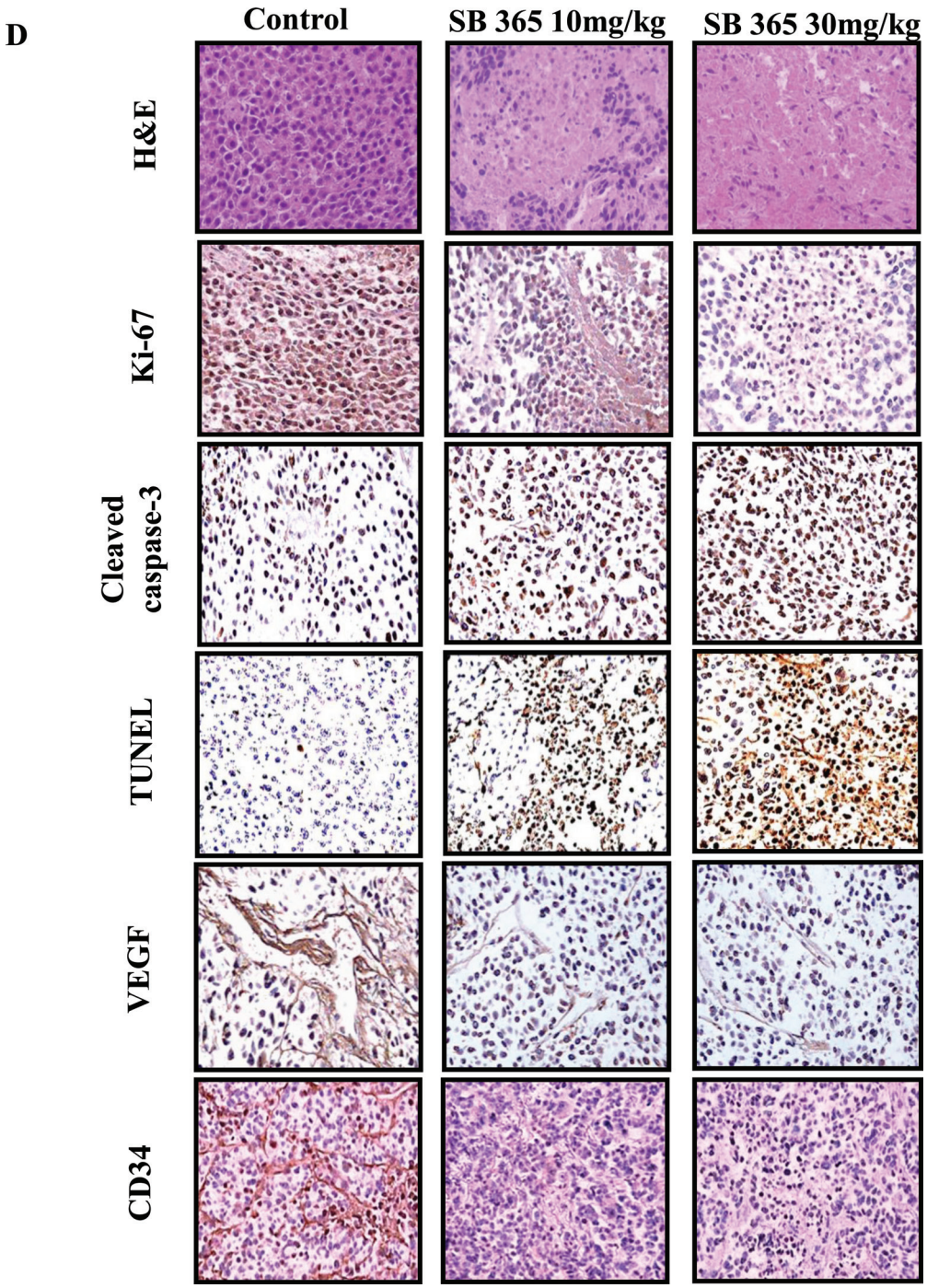

SB365 inhibited HGF-induced microvessel sprouting ex vivo and a Matrigel plug assay in vivo

We further explored the antiangiogenic activity of SB365 using *ex vivo* and *in vivo* angiogenesis models. First, to investigate whether SB365 inhibited HGF-induced angiogenesis *ex vivo*, we examined the sprouting of vessels from aortic rings in the presence or absence of SB365. HGF (100 ng/ml) significantly stimulated microvessel sprouting, leading to the formation of a meshwork of vessels around the aortic rings ($P < 0.05$, Figure 4D). Treatment with SB365 dramatically inhibited HGF-induced sprouting from the aortic rings, and 10 μM SB365 almost completely inhibited sprouting. Next, we used the Matrigel plug assay to confirm the effects of SB365 on HGF-inducted angiogenesis *in vivo*. Matrigel containing HGF with or without SB365 was subcutaneously injected into male BALB/c mice. After 7 days, Matrigel plugs containing HGF alone appeared red due to the presence of red blood cells, indicating that new blood vessel vasculature had formed inside the Matrigel via angiogenesis triggered by HGF (Figure 5A). However, the addition of 10 μM SB365 to the Matrigel plugs considerably inhibited vascular formation. For histological analysis, each section of the Matrigel plug was stained with hematoxylin and eosin and CD34, respectively. The stained Matrigel sections showed fewer vessels in the plug containing SB365 than in the HGF-induced Matrigel plug. Expression of CD34 was also decreased upon SB365 inclusion in the HGF-induced Matrigel plug. These results confirmed that SB365 has potent antiangiogenic activity *in vivo* (Figure 5A and B).

SB365 inhibited the activation of the HGF-induced c-Met and VEGF in MKN-45 gastric cancer cell and HUVECs

In the vasculature, c-Met activation via HGF plays an important role in regulating tumor angiogenesis (29). Further, HGF is reported to

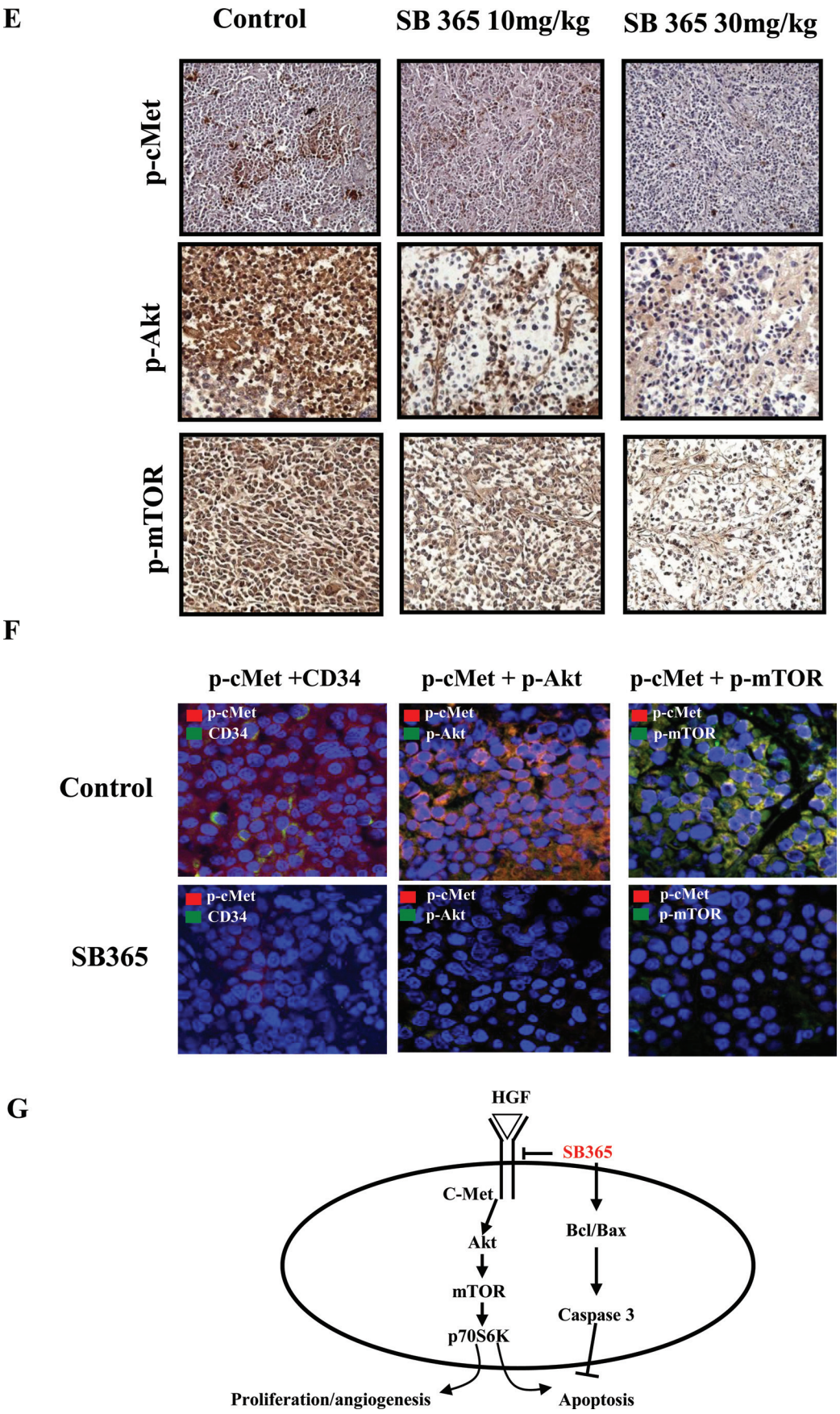

Fig. 6. *In vivo* effect of SB365 in the hepatocellular carcinoma mouse xenograft model. (**A**) Tumor growth of MKN-45 cells xenograft in nude mice. (**B**) Average body weight of nude mice. All mice were implanted by subcutaneous injection of MKN-45 cells (5×10^6 cells/200 µl PBS) on the flank. (**C**) Tumor size and weight in MKN-45 mouse xenograft. Data are represented by mean ± SD ($n = 6$). *$P < 0.05$ and **$P < 0.01$, compared with control. (**D**) Effect of SB365 on proliferation,

promote angiogenesis with the upregulation of VEGF (30). So, we investigated whether SB365 inhibits HGF-induced c-Met and VEGF in both gastric cancer and HUVECs. As shown in Figure 5C and D, SB365 inhibited HGF-induced c-Met and VEGF expression in MKN-45 gastric cancer cells. Additionally, in HUVECs, SB365 inhibited HGF-induced VEGF expression. These results show that SB365 may block the HGF/c-Met interaction in tumor angiogenesis.

SB365 suppressed tumor growth in a gastric cancer xenograft model together with in vivo antiproliferative, antiangiogenic and apoptotic effects

Based on the above *in vitro* findings, we extended our study to an *in vivo* xenograft model. After inoculation with MKN-45 gastric cancer cells, mice were daily administrated by oral gavage with SB365 at doses of 10 or 30 mg/kg for 12 days. SB365 treatment showed inhibition of tumor growth on the third day of treatment, and tumor growth inhibition became more visible and significant at both doses on 10 and 30 mg/kg on the ninth day of treatment, compared with controls (Figure 6A). Consistent with this observation, the weight of the tumors isolated from the SB365-treated groups decreased ~50 and 60% at doses of 10 and 30 mg/kg, respectively, relative to the control (Figure 6C, $P < 0.01$). No adverse effects or significant changes in body weight were observed in animals treated with SB365, compared with the control animals, indicating that SB365 has no obvious toxicity to mice at doses that caused tumor regression (Figure 6B). In histopathology analysis by a special pathologist, MKN-45 tumors were characterized by poorly differentiated adenocarcinoma, where cells were in patchy, nestle or streaky arrangement and shaped round, oval or irregular. Cell differentiation was poor, with large deep-stained nuclei and a large nuclear–cytoplasmic ratio, which were similar with those of human gastric cancer tissues. However, the treatment of SB365 suppressed these pathological problems in a dose-dependent manner.

To further assess whether SB365 inhibits tumor growth through the inhibition of tumor angiogenesis and proliferation, and the induction of apoptosis, we evaluated the expression of Ki-67, TUNEL, cleaved caspase-3, VEGF and CD34, along with p-Met, p-Akt and p-mTOR, in the tumor tissues. As shown in Figure 6D, SB365 treatment resulted in the decreased expression of Ki-67, VEGF and CD34 in the SB365-treated group as compared with the control group. In addition, the apoptotic effect of SB365 on gastric tumor tissues was observed in the increased expression of the cleaved caspase-3 and DNA fragments using the TUNEL assay. Furthermore, SB365 treatment decreased the phosphorylation of c-Met, Akt and mTOR, indicating the regulation of many different events involved in cell survival and proliferation (Figure 6E and F). Taken together, our results demonstrate that SB365 has potent antitumor efficacy in gastric cancer xenograft models.

Discussion

The focus in cancer control has been on the search for anticancer agents, which are safer and have higher patient acceptability. For this reason, various natural agents such as phytochemicals, components of the human diet or traditional herbal medicine have been examined. In the present study, we isolated SB365, a new saponin D from *P.koreana*. Accumulated evidences suggest that various saponins have chemopreventive or chemotherapeutic effects on cancer (16–18). Based on previous studies, we set out to identify the anticancer effects of saponin D SB365 and its mechanism of action against gastric cancer. Here, we report for the first time that SB365 docks at an allosteric site in c-Met, and thereby target the c-Met signaling pathway, which may lead to the inhibition of cell growth and angiogenesis together with the induction of apoptosis in gastric cancer.

Phytochemicals with precisely defined mechanisms of action based on molecular target identification can be linked to successful drug discovery. Previously, several phytochemicals, including resveratrol (31), epigllocatechin gallate (32), gingerol (33) and myricetin (34), have been reported to directly modulate various molecular signal transduction pathways. Such research efforts have centered on the effects of phytochemicals on signaling cascades that are known to induce cancer cell death or inhibit cancer cell proliferation. However, specific molecular and cellular targets need to be identified. In this study, to better understand the anticancer effects of SB365 in the view of target mechanism, we firstly used an RTK array. We found that among the 42 RTKs, tested, SB365 effectively inhibited the phosphorylation of c-Met, which is extensive in MKN-45 gastric cancer cells. Based on this observation, we attempted to establish a binding model of the c-Met–SB365 complex to explore how SB365 interacts with c-Met, using X-ray crystallographic structures and molecular modeling techniques. Interestingly, SB365 docked into an allosteric site in c-Met that is created by an inactive 'DFG-out' conformation, suggesting that SB365 is an allosteric inhibitor of c-Met. Most known kinase inhibitors are type I inhibitors, adenosine triphosphate (ATP)-competitive compounds, that bind in the ATP-binding site and hydrogen bond with the hinge region of the kinase (35). However, such inhibitors have shown problems such as limited selectivity and drug resistance (36,37). Recently, type II inhibitor compounds (non-ATP-competitive inhibitors), which bind at an allosteric site that is present only in the inactive ('DFG-out') kinase conformation, have been shown to posses advantageous pharmacological properties (38). Indeed, the identification of allosteric inhibitors that stabilize inactive kinase conformations is expected to provide valuable insights into the development of new chemical agents to address the most defined current challenges in kinase drug discovery (39). We, therefore, investigated whether SB365 is more effective than PF-02341066, a potent c-Met inhibitor (crizotinib, an ATP-competitive inhibitor) in various c-Met alterations cells. PF-02341066 only inhibited cell growth in c-Met-amplified-MKN-45 cells, whereas SB365 equally inhibited cell growth in all MKN-45, NCI-H596 (c-Met splicing mutation) and HT-29 (c-Met overexpression) cells (IC_{50} = 1–2 μM c-Met inhibition). Inhibition effect of PF-02341066 in c-Met amplification cells has been observed in study of Okamoto *et al.* (40) that PF-02341066 showed a marked antitumor action specifically positive for c-Met amplification in gastric cancer cells. Based on the above results and previous study, we propose that SB365 may be a potential natural inhibitor of c-Met.

Within cancer, c-Met is a well-established mediator of carcinogenesis. Under physiological conditions, c-Met is activated by its ligand, HGF, to induce an invasive program consisting of cell proliferation, migration, invasion and survival (29,41). Following c-Met phosphorylation and activation, multiple signaling pathways are involved as downstream targets, such as the PI3K/Akt/mTOR, STAT3 and Ras/Mek pathways (24–26). Therefore, to elucidate the mechanism of c-Met inhibition by SB365, we investigated whether SB365 inhibited the expression of p-Akt, p-STAT3 and p-Mek, which are representative downstream molecules of the PI3K/Akt/mTOR, JAK/STAT3 and Ras/Mek signaling pathways. Among those, SB3365 most notably inhibited the expression of p-Akt in MKN-45 gastric cancer cells. In addition, SB365 inhibited the phosphorylations of Akt and mTOR as well as the downregulation of p70S6K, the main mediators of the PI3K/Akt/mTOR signaling pathway in MKN-45 gastric cancer cells. Indeed, Wang *et al.* (42) has reported that constitutive activation of c-Met may be a vital contributor to the activation of the PI3K/Akt pathway. Furthermore, aberrant HGF/c-Met signaling induces centrosome amplification via the PI3K/Akt pathway (43). In addition, c-Met activation prevents apoptosis through PI3K activation and subsequent Akt activation (44,45). Based on the above studies, we hypothesized that the anticancer effect of SB365 is associated

←
apoptosis and angiogenesis of gastric cancer xenograft. Tumors were excised and processed for immunostaining for Ki-67, cleaved caspase-3, TUNEL, VEGF and CD34 including hematoxylin and eosin staining. (**E**) Expression of p-cMet and p-Akt by SB365 in tumor tissues. (**F**) Immunofluorescence staining for expression of p-cMet, CD34, p-Akt and p-mTOR by SB365 in tumor tissues (×400 magnification). (**G**) Schematic model showing the anticancer effect of SB365 in gastric cancer.

with the regulation of the c-Met/Akt/mTOR pathway. Indeed, our study showed that SB365 inhibited expression of p-cMet, p-Akt and p-mTOR together with inhibition of tumor growth and induction of apoptosis in gastric cancer xenograft models (Figure 6G). Accordingly, the antitumor efficacy of SB365 is likely mediated by c-Met inhibition through the PI3K/Akt/mTOR signaling pathway.

Another major mechanism by which SB365 mediates anticancer effects against gastric cancer appears to be the suppression of angiogenesis. The HGF/c-Met pathway is known to promote tumor angiogenesis thereby fostering cancer progression (46). Ponzo *et al.* (46) have reported that c-Met is expressed in endothelial cells and that HGF can stimulate endothelial cell growth, invasion and motility. Also, inhibition of c-Met activity impairs the survival, invasion and tubulogenesis of HUVECs *in vitro* and reduces neovascularization and microvessel formation in tumor models (47,48). In accordance with this evidence, our results showed that SB365 at the low concentration of 0.1 μM could effectively inhibit endothelial cell migration and capillary structure formation in HGF stimulation models *in vitro*. Additionally, SB365 possessed antiangiogenic activity, strongly inhibiting HGF-induced microvessel sprouting and new vessel formation in the Matrigel plug assay. Furthermore, SB365 inhibited HGF-induced c-Met and VEGF expression in MKN-45 gastric cancer cells and HGF-induced VEGF expression in HUVECs. Previous studies have reported that HGF promotes angiogenesis via the upregulation of VEGF (30). Loss of HGF signaling has been reported to reduce VEGF expression or its angiogenic potency (49). In this sense, we think it is noteworthy that SB365 inhibited HGF-mediated c-Met and VEGF expression. Taken together, these observations show that SB365 may account for blocking the HGF/c-Met interaction in the process of tumor angiogenesis.

In conclusion, our results show that SB365 regulated c-Met expression as an inhibitor of c-Met docking into an allosteric site of c-Met. Furthermore, we have demonstrated that SB365 can suppress tumor growth and angiogenesis and induce apoptosis by downregulation of c-Met activation through the PI3K/Akt/mTOR signaling pathway *in vitro* and *in vivo* in gastric cancer. Our discovery of this novel anticancer mechanism of SB365 not only confirms its ethnopharmacological value but also may contribute to modern drug development.

Supplementary material

Supplementary Materials and methods can be found at http://carcin.oxfordjournals.org/

Funding

Korean Health Technology R&D Project (A120266, A110944); Ministry of Health and Welfare; the National Research Foundation of Korea (NRF) funded by the Ministry of Education, Science and Technology (NRF-2012-0002988, 2012R1A2A2A01045602, 2012R1A1A2043281) and Inha University Grant.

Conflict of Interest Statement: None declared.

References

1. Crew,K.D. *et al.* (2006) Epidemiology of gastric cancer. *World J. Gastroenterol.*, **12**, 354–362.
2. Maehara,Y. *et al.* (1991) Pertinent risk factors and gastric carcinoma with synchronous peritoneal dissemination or liver metastasis. *Surgery*, **110**, 820–823.
3. Moriguchi,S. *et al.* (1992) Risk factors which predict pattern of recurrence after curative surgery for patients with advanced gastric cancer. *Surg. Oncol.*, **1**, 341–346.
4. Bottaro,D.P. *et al.* (1991) Identification of the hepatocyte growth factor receptor as the c-met proto-oncogene product. *Science*, **251**, 802–804.
5. Christensen,J.G. *et al.* (2005) c-Met as a target for human cancer and characterization of inhibitors for therapeutic intervention. *Cancer Lett.*, **225**, 1–26.
6. Di Renzo,M.F. *et al.* (1991) Expression of the Met/HGF receptor in normal and neoplastic human tissues. *Oncogene*, **6**, 1997–2003.
7. Comoglio,P.M. *et al.* (2008) Drug development of MET inhibitors: targeting oncogene addiction and expedience. *Nat. Rev. Drug Discov.*, **7**, 504–516.
8. Liu,X. *et al.* (2008) Targeting the c-MET signaling pathway for cancer therapy. *Expert Opin. Investig. Drugs*, **17**, 997–1011.
9. Zeng,Z.S. *et al.* (2008) c-Met gene amplification is associated with advanced stage colorectal cancer and liver metastases. *Cancer Lett.*, **265**, 258–269.
10. Seiwert,T.Y. *et al.* (2009) The MET receptor tyrosine kinase is a potential novel therapeutic target for head and neck squamous cell carcinoma. *Cancer Res.*, **69**, 3021–3031.
11. Knowles,L.M. *et al.* (2009) HGF and c-Met participate in paracrine tumorigenic pathways in head and neck squamous cell cancer. *Clin. Cancer Res.*, **15**, 3740–3750.
12. Toiyama,Y. *et al.* (2009) Serum hepatocyte growth factor as a prognostic marker for stage II or III colorectal cancer patients. *Int. J. Cancer*, **125**, 1657–1662.
13. Inoue,T. *et al.* (2004) Activation of c-Met (hepatocyte growth factor receptor) in human gastric cancer tissue. *Cancer Sci.*, **95**, 803–808.
14. Wang,J.Y. *et al.* (2004) Alterations of APC, c-met, and p53 genes in tumor tissue and serum of patients with gastric cancers. *J. Surg. Res.*, **120**, 242–248.
15. Corson,T.W. *et al.* (2007) Molecular understanding and modern application of traditional medicines: triumphs and trials. *Cell*, **130**, 769–774.
16. Bang,K.H. (1999) *The Medicinal Plant of Korea*. Kyo-Hak Press, Seoul, Korea, p. 139.
17. Price,K.R. *et al.* (1987) The chemistry and biological significance of saponins in foods and feedingstuffs. *Crit. Rev. Food Sci. Nutr.*, **26**, 27–135.
18. Taylor,W.G. *et al.* (2000) Microdetermination of diosgenin from fenugreek (*Trigonella foenum-graecum*) seeds. *J. Agric. Food Chem.*, **48**, 5206–5210.
19. Vincken,J.P. *et al.* (2007) Saponins, classification and occurrence in the plant kingdom. *Phytochemistry*, **68**, 275–297.
20. Haridas,V. *et al.* (2001) Avicins: triterpenoid saponins from *Acacia victoriae* (Bentham) induce apoptosis by mitochondrial perturbation. *Proc. Natl Acad. Sci. USA*, **98**, 5821–5826.
21. Mujoo,K. *et al.* (2001) Triterpenoid saponins from *Acacia victoriae* (Bentham) decrease tumor cell proliferation and induce apoptosis. *Cancer Res.*, **61**, 5486–5490.
22. Qian,F. *et al.* (2009) Inhibition of tumor cell growth, invasion, and metastasis by EXEL-2880 (XL880, GSK1363089), a novel inhibitor of HGF and VEGF receptor tyrosine kinases. *Cancer Res.*, **69**, 8009–8016.
23. Diller,D.J. *et al.* (2001) High throughput docking for library design and library prioritization. *Proteins*, **43**, 113–124.
24. Recio,J.A. *et al.* (2002) Hepatocyte growth factor/scatter factor activates proliferation in melanoma cells through p38 MAPK, ATF-2 and cyclin D1. *Oncogene*, **21**, 1000–1008.
25. Zhang,Y.W. *et al.* (2002) Requirement of Stat3 signaling for HGF/SF-Met mediated tumorigenesis. *Oncogene*, **21**, 217–226.
26. Ponzetto,C. *et al.* (1994) A multifunctional docking site mediates signaling and transformation by the hepatocyte growth factor/scatter factor receptor family. *Cell*, **77**, 261–271.
27. Yap,T.A. *et al.* (2008) Targeting the PI3K-AKT-mTOR pathway: progress, pitfalls, and promises. *Curr. Opin. Pharmacol.*, **8**, 393–412.
28. Huang,L.E. *et al.* (1998) Regulation of hypoxia-inducible factor 1alpha is mediated by an O2-dependent degradation domain via the ubiquitin-proteasome pathway. *Proc. Natl Acad. Sci. USA*, **95**, 7987–7992.
29. Birchmeier,C. *et al.* (2003) Met, metastasis, motility and more. *Nat. Rev. Mol. Cell Biol.*, **4**, 915–925.
30. Zhang,Y.W. *et al.* (2003) Hepatocyte growth factor/scatter factor mediates angiogenesis through positive VEGF and negative thrombospondin 1 regulation. *Proc. Natl Acad. Sci. USA*, **100**, 12718–12723.
31. Zykova,T.A. *et al.* (2008) Resveratrol directly targets COX-2 to inhibit carcinogenesis. *Mol. Carcinog.*, **47**, 797–805.
32. Ermakova,S.P. *et al.* (2006) (−)-Epigallocatechin gallate overcomes resistance to etoposide-induced cell death by targeting the molecular chaperone glucose-regulated protein 78. *Cancer Res.*, **66**, 9260–9269.
33. Jeong,C.H. *et al.* (2009) [6]-Gingerol suppresses colon cancer growth by targeting leukotriene A4 hydrolase. *Cancer Res.*, **69**, 5584–5591.
34. Jung,S.K. *et al.* (2010) Myricetin inhibits UVB-induced angiogenesis by regulating PI-3 kinase *in vivo*. *Carcinogenesis*, **31**, 911–917.
35. Liu,Y. *et al.* (2006) Rational design of inhibitors that bind to inactive kinase conformations. *Nat. Chem. Biol.*, **2**, 358–364.
36. Jabbour,E. *et al.* (2006) Novel tyrosine kinase inhibitors in chronic myelogenous leukemia. *Curr. Opin. Oncol.*, **18**, 578–583.
37. Zhang,J. *et al.* (2009) Targeting cancer with small molecule kinase inhibitors. *Nat. Rev. Cancer*, **9**, 28–39.

38. Kufareva,I. *et al.* (2008) Type-II kinase inhibitor docking, screening, and profiling using modified structures of active kinase states. *J. Med. Chem*., **51**, 7921–7932.
39. Simard,J.R. *et al.* (2009) A new screening assay for allosteric inhibitors of cSrc. *Nat. Chem. Biol*., **5**, 394–396.
40. Okamoto,W. *et al.* (2012) Antitumor action of the MET tyrosine kinase inhibitor crizotinib (PF-02341066) in gastric cancer positive for MET amplification. *Mol. Cancer Ther*., **11**, 1557–1564.
41. Corso,S. *et al.* (2005) Cancer therapy: can the challenge be MET? *Trends Mol. Med*., **11**, 284–292.
42. Wang,K. *et al.* (2012) Inhibition of c-Met activation sensitizes osteosarcoma cells to cisplatin via suppression of the PI3K-Akt signaling. *Arch. Biochem. Biophys*., **526**, 38–43.
43. Nam,H.J. *et al.* (2010) The PI3K-Akt mediates oncogenic Met-induced centrosome amplification and chromosome instability. *Carcinogenesis*, **31**, 1531–1540.
44. Derksen,P.W. *et al.* (2003) The hepatocyte growth factor/Met pathway controls proliferation and apoptosis in multiple myeloma. *Leukemia*, **17**, 764–774.
45. Xiao,G.H. *et al.* (2001) Anti-apoptotic signaling by hepatocyte growth factor/Met via the phosphatidylinositol 3-kinase/Akt and mitogen-activated protein kinase pathways. *Proc. Natl Acad. Sci. USA*, **98**, 247–252.
46. Ponzo,M.G. *et al.* (2009) Met induces mammary tumors with diverse histologies and is associated with poor outcome and human basal breast cancer. *Proc. Natl Acad. Sci. USA*, **106**, 12903–12908.
47. Zou,H.Y. *et al.* (2007) An orally available small-molecule inhibitor of c-Met, PF-2341066, exhibits cytoreductive antitumor efficacy through antiproliferative and antiangiogenic mechanisms. *Cancer Res*., **67**, 4408–4417.
48. Heideman,D.A. *et al.* (2004) Suppression of tumor growth, invasion and angiogenesis of human gastric cancer by adenovirus-mediated expression of NK4. *J. Gene Med*., **6**, 317–327.
49. Xin,X. *et al.* (2001) Hepatocyte growth factor enhances vascular endothelial growth factor-induced angiogenesis *in vitro* and *in vivo*. *Am. J. Pathol*., **158**, 1111–1120.

Received September 20, 2012; revised April 26, 2013; accepted May 7, 2013